Activated gallic acid as radical and oxygen scavenger in biodegradable packaging film

Fabio Di Giuseppe, Fanny Coffigniez, Chahinez Aouf, Valérie V. Guillard, Elena Torrieri

Activated gallic acid as radical and oxygen scavenger in biodegradable packaging film

Fabio di Giuseppe[1], Fanny Coffigniez[2*], Chahinez Aouf[2], Valérie Guillard[2], Elena Torrieri[1]

Food packaging and shelf life

[1]Department of Agricultural Sciences, University of Naples "Federico II", Via Università 100, 80055 Portici (NA), Italy

[2] IATE, Agro polymers Engineering & Emerging Technology, Univ Montpellier, INRAE, Institut Agro, Montpellier & CIRAD, Montpellier, France

* Corresponding author: Fanny Coffigniez, IATE, 2 place Pierre Viala, Bat 31, 34060 Montpellier, France. E-mail: fanny.coffigniez@umontpellier.fr ; phone: ++33 (0) 499 613 021

Abstract

A coupled experimental and modelling approach was developped to characterize the radical inhibition and oxygen scavenger properties of gallic acid/ sodium carbonate mixture included in a PHBV film. PHBV active packaging was produced by thermoforming. In contact with acqueous and fatty food simulants, almost 30% of the initial gallic acid was released into food simulants A (10% ethanol), and D1 (50% ehtanol), where it showed a radical inhibition value (I%) reaching 68±0.1% and 77±0.1% respectively, while no release was observed in food simulant D2 (isooctane). In addition, the active films displayed an O_2 scanvenger capacity of 120 mg O_2 g^{-1} GA at room temperature, after 10 days of storage. Models showed a good fitting to experimental data. The PHBV active packaging combining both antiradical and oxygen scavenger activities has high potential for food protection. However, some improvements are still needed to enhance its oxygen barrier capacity and to meet the reglementation.

Keywords: active packaging, biodegradable polymer, O_2 scavenger, antiradical, O_2 scavenging modelling

1.Introduction

Nowadays, one major challenge is to develop a sustainable packaging with low environmental impact, able to preserve food quality and safety. The use of biobased and biodegradable packaging is a way to reduce both the exploitation of fossil resources and the accumulation of plastic waste, thus preventing the environmental and health problems that result from this (Cazón et al., 2017; Guillard et al., 2018; Mohamed et al., 2020).

In addition, this biodegradable packaging should also be able to preserve the quality of food and extend its shelf life in order to reduce food waste and prevent food-borne deseases (Angellier-Coussy et al., 2013; Coffigniez et al., 2021). Oxidation is one of the major food degradations. It is responsible for structural alterations, producing off-flavors, discoloration and loss of nutritional quality and safety due to the formation of potentially toxic secondary compounds (lipid and protein oxydation), thus making foods unsuitable for consumption (Gómez-Estaca et al., 2014; Hellwig, 2019). One way to limit these oxidation reactions is the use of active packaging containing antioxidants that can diffuse into the food or act as oxygen absorbers by maintaining an oxygen-free atmosphere (Vermeiren et al., 1999).

To be used in food packaging, antioxidants should meet certain criteria. They have to (i) be safe; (ii) effective at low concentrations and (iii) not modify odor, color and flavor of the product and (iv) above all, should comply with food and packaging regulation into force. Due to their good antioxidant activity, natural phenolic compounds seem to be ideal candidates for integration into a fully biobased and biodegradable system (Sanches-Silva et al., 2014). Diffent studies dealing with the incorporation of phenolic compounds into biobased films to extend the food shelf life have been reported (Wang et al., 2019; Radi et al., 2017; Carrizo et al., 2016; Licciardello et al., 2015).

Gallic acid (2,3,4-trihydroxybenzoic acid) (GA), a phenolic acid present in different parts of superior plants such as bark, wood, leaf, root and seed (Luzi et al., 2019; Campo et al., 2016) has the particularity of having three phenolic hydroxyl groups in the ortho position, which increases its antioxidant activity. By means of electrospinning, GA was encapsulated into lentil

flour/polyethylene oxide and methylcellulose/polyethylene oxide nanofibers. Due to the release of GA into walnuts, the resulting materials led to the decrease of their peroxide value by half at 40°C for 21 days of storage (Aydogdu et al., 2019).

The oxygen scavenging ability of GA was investigated by Wanner, G. T. (2010), Ahn et al., (2016); Pant et al., (2017) and Singh et al., (2020) who showed that GA combined to alkaline molecules (sodium carbonate, sodium hydroxide or potassium chloride) had a strong oxygen absorption capacity when it was incroporated in low density polyethylene film; bio-based mulitlayer film and chitosan film respectively. In the presence of a base, the oxygen scavenger activity of gallic acid is activated by humidity derived from the product or the environnement. Indeed, GA is a weak polyprotic acid with four acidic protons. As a function of the medium pH, different gallate anions can be formed. In the presence of dissolved oxygen, the autooxidation mechanism gives rise to gallate radicals by electron transfer or hydrogen atom transfer. This process leads to the formation of several GA autooxidation intermediates, along with the absorption of oxygen (Pant et al., 2019; Wanner, 2010). Accurate determination of the O_2 absorption capacity and absorption rate is a prerequisite to modelling approach of the oxyen diffusion – reaction in material containing antioxidants. Modelling of such activity is important to design efficient system well targeted to the intended application as food packaging, as it was previously applied on iron based scavenging films for instance (Kombaya-Touckia-Linin et al., 2019). However, this approach was never carried out on gallic acid based scavenging films.

Poly(3-hydroxybutyrate-co-3hydroxyvalerate) communly known as PHBV is a biobased polyester belonging to the wide family of polyhydroxyalkanoate polymers. It displays good barrier properties and its physical properties are similar to some fossil-derived polymers such as polypropylene. Furthermore, it is non toxic, biocompatible and biodegradable in natural conditions (Berthet et al., 2015; Bossu et al., 2020). To the best of our knowledge, the design of an active packaging based on the PHBV/GA system, which could combine oxygen scavenging (by absorbing atmospheric oxygen) and radical scavenging (by migrating into food) activities, has never been studied before.

In the present work, PHBV film containing 5wt% of activated GA was produced. The antioxidant activity of GA as both radical and oxygen scavenger was deeply investigated and a diffusion-reaction mathematical model was applied to predict the oxygen scavenger activity of the active packaging. This is the first time that such complete experimental and modelling approach was carried out on GA-based material targeting both antioxydant and oxygen scavenger activities.

2. Materials and Methods

2.1 Materials

Gallic acid monohydrate (GA) and sodium carbonate (Na_2CO_3) were purchased from abcr Gmbh and Geyer (Germany) respectively. Tianan (China) commercial grades of poly (3-hydroxybutyrate-co-3-hydroxyvalerate) with 3 wt% of 3HV (P(3HB-co-3HV)) in the form of pure uncompounded powder with no additive, was purchased from Natureplast (France). Ultrapure water was obtained from a Millipore Milli-Q system (Millipore, Bedford, MA, USA). 2,2-diphenyl-1-picryl-hydrazyl radical (DPPH), ethanol 96%, methanol 99%, formic acid 96%, acetonitrile 99.9% and isooctane (for synthesis) were purchased from Sigma Aldrich France.

2.2 Preparation of the active film: compounding and thermoforming

PHBV, GA and Na_2CO_3 powders were separately dried at 60 °C for at least 48 h before using. PHBV powder containing 5% (w/w) of GA and 2.5% (w/w) of Na_2CO_3 (weight ratio of 2:1) was mixed and melt-blendeded using a co-rotating twin-screw microextruder (model “process 11” thermofisher). The screw speed was set at 200 rpm and the barrel temperature profile to 180°C (from top to bottom). The residence time was 1.5 min. The melt strain was cooled down at room temperature (and air conditions) and pelletized (Pelletizer from Thermofischer, Germany). After drying during one night at 60°C under vacuum, the pellets were transformed into films by means of an hydraulic thermopress (CFM 20T, Pinette Emidecau Industries, Chalon sur Saone cedex, France)

122 at 180°C. Pellets were melt for 1 min at 5 bar, then 1 min at 150 bar. The film was cooled down
123 using a cold bath water on the surface of the metal form used to produce the films (in air
124 conditions). The average thickness of the realized films used for evaluation of migration, radical
125 and scavenging properties and for microscopic analysis were about 357.5±10.5 µm and 206.1±20.7
126 µm respectively. The final GA-PHBV films were stored in hermatically box free of oxygen until
127 use.
128
129 **2.3 Determination of the film properties**
130 **2.3.1 Evaluation of GA recovery and distribution in the film after thermoforming**
131 **2.3.1.1 From macroscopic point of view**
132 PHBV/GA sheets of 144 cm^2 was divided into four equal parts and GA contained in each part was
133 quantified after extraction, at 25°C, during 18 h using methanol as solvent. The amount of GA was
134 determined thanks to UV quantification in an Aquity UPLC (Waters, Milford, MA) liquid
135 chromatography system, equipped with a photodiode array detector (DAD). The Waters column
136 was 100mm x 2.1mm, HSS T3, with 1.8µm particles size. Solvents used were A (99% H_2O and
137 1%HCOOH v/v) and B (80% CH_3CN, 19.9% H_2O and 0.1% HCOOH) with a flow rate of
138 0.55mL/min. The gradient conditions were as follows: from 0 to 5 min, 99% to 60% A; from 5 min
139 to 7 min, 60% to 1% A; from 7 min to 8 min, 1% A; from 8 min to 9 min, 1% to 99.9% A. The
140 injection volume was 2 µl, DAD was set at 280 nm, and gallic acid was detected at 1.5 min
141 retention time (Rouméas et al., 2018). GA was quantified after external calibration with GA for
142 standard dissolved in methanol.
143
144 **2.3.1.2 From microscopic point of view**
145 PHBV/GA films of 1 cm width and 200µm thickness (thinner films were used for this analysis)
146 were observed with a wide-field microscope Eclipse Ni-E (Nikon Instruments Inc, NY, USA) with

147 filter cube UV-2A, exc: 330-380, em: 420-800. The pictures were obtained with the 10X Plan APO
148 objective and a Nikon CMOS DS-Ri2 camera. They were processed with Image J v1.8.0 software.
149
150 **2.3.2 GA migration into food simulants**
151 Three food simulants were selected to study the GA migration, namely, simulant A (10% ethanol)
152 corresponding to aqueous food, simulant D1 (50% ethanol) corresponding to alcoholic food (above
153 20% of alcohol) and oil in water emulsion and simulant D2 (vegetable oil was replaced by
154 isooctane) corresponding to food containing free fats on the surface (European Standard EN
155 10/2011, (European Commission, 2011). Migration studies were conducted in triplicate at 25°C
156 over 10 days in a climatic chamber (Memmert, Germany). Double-sided, total immersion migration
157 tests were performed with 60 cm^2 of films and 100 mL of each simulant (area-to-volume ratio
158 around 6 dm^2/L). A blank test for each simulant was also carried out. Extracts (1 mL) were
159 collected each day and GA concentration in food simulant was quantified by UPLC, as previously
160 mentioned in section 2.3.2.1.
161 To estimate the corresponding percentage of GA diffused in food simulant, the following equation
162 was used:
163 $$\%\ \text{of GA diffused in food simulant} = \frac{C_x \times V_{FS}}{m_f \times \%GA} \quad (1)$$
164 With, C_x the mass concentration of GA (mg/L), V_{FS} the volume of food simulant (L), m_f the mass
165 of film (mg) and $\%GA$ the percentage of GA included in the PHBV film (5 wt %).
166
167 **2.3.3 Radical scavenger activity of released GA into food simulants**
168 The DPPH assay consists in measuring the ability of a molecule to reduce the 2,2-diphenyl-1-
169 picryl-hydrazyl radical (DPPH·) in methanol, resulting in its bleaching at 517 nm. The scavenging
170 activity of GA against DPPH· was performed spectrometrically at 517 nm and 30°C, according to
171 (Laguna et al., 2020). Solutions containing 100 µL of each food simulant collected at each time

(with GA concentrations from 8 to 54 mg/L) and 100 µL of DPPH methanolique solution (40 mg/L) were poured into Humidity cassette microplates (TEC96ft_cell Tecan 96Flat Transparent). The absorbance decay was monitored each 2 minutes until it reached a steady state (15 min). The spontaneous bleaching of DPPH˙was also measured in absence of antioxidant (blank). All the determinations were performed in duplicate. The percentage inhibition values (I%) were calculated using the following equation:

$$I\% = \frac{Abs_c - Abs_s}{Abs_c} \times 100 \quad (2)$$

where Abs_c is the absorbance of pure DPPH and Abs_s is the absorbance of the sample.

2.3.4 Oxygen scavenger properties of active component and active film

The oxygen scavenger capacity of the active mixture composed of GA and Na_2CO_3 in ratio 2:1 in both powder form and inclusion in polymer matrix was determined according to DIN 6139 at 23°C and 100% RH (Pant et al., 2017). The active mixture (0.3 g of GA and 0.17 g of Na_2CO_3 for powder mixture or 5.8g of film pieces containg 5% of GA and 2.5% of Na_2CO_3 for inclusion polymer matrix) were stored in hermetically closed glass cells (V=514 cm^3) equipped with steel lid. The saturated humidity was assured by distilled water (50 mL) put in a glass bowl at the bottom of the cell. The O_2 depletion in the headspace (initial gas atmosphere: air) during storage was determined non-destructively using a luminescence-based oxygen detection system (PreSens Precision Sensing GmbH, Regensburg, Germany) with an optical sensor spot stuck on the underside of the cell wall. The O_2 partial pressure in the cell was monitored over time and the cell was briefly reopened to regenerate the oxygen at 20.9% when it became zero. The experiment conducted in triplicate, was stopped when the maximum absorption capacity was reached, i.e. when no decrease of oxygen partial pressure has been detected. The O_2 absorption quantity (mg O_2) was calculated from the O_2 partial pressure depletion, using the following equation:

$$m_{O_2} = \frac{P_{O2} \times V_{HS} \times M_{O2}}{R \times T} \quad (3)$$

Where m_{O_2} is the oxygen content absorbed into the system (g), R=8.314 Pa m^3 mol^{-1} K^{-1} is the gas ideal constant, T is the temperature (K), V_{HS} is the headspace volume of the cell (m^3) and M_{O2} is the oxygen molar mass (g mol^{-1}). The oxygen absorption capacity of active compound film was calculated in mg of absobed O_2 per gram of gallic acid.

2.3.5 Oxygen permeability of the active film

Active film (with 357.5±10.5 µm thickness) was cut into circles with 12.5 cm^2 diameter and their oxygen permability (mol m^{-1} s^{-1} Pa^{-1}) was measured at 23°C and 50% RH using an oxygen permeation cell (OTR, PresSens-GmbH, Germany) according to a modified ASTM Standard (2007) procedure. The oxygen partial pressure in the upper chamber was measured using an optical luminescence quenching method (Presens, GmbH).

The oxygen permeability coefficient PO_2 (mol m^{-1} s^{-1} Pa^{-1}) was determined as reported in the following equation:

$$PO_2 = \frac{\dot{P} \times l}{A \times P_{atm}} \quad (4)$$

Where $\dot{P}$ (mol s^{-1}) is the slope of the oxygen partial pressure increase in the upper chamber, A (m^2) and l (m) are the surface and the average thickness of the film respectively. P_{atm} is the standard atmosphere pressure. The thickness of the film was determined at five different points of the film using a micrometer (Mitutoyo).

2.4 Mathematical models development

2.4.1 Modeling of the apparent diffusion of GA in the PHBV film

Assuming that : (i) the film is a one dimensionnal infinite plane sheet with an homogeneous thickness, (ii) GA is homogeneously distributed in the PHBV film and in food simulant (if GA diffused in food simulant) and (iii) the film does not swell during the process; the estimation of the

gallic acid apparent diffusivity (D_{app}) in the PHBV film was made using an analytical solution of the Fick's second law (equation (5)) as described by Lajarrige et al., (2019).

$$\frac{M_t}{M_\infty} = 1 - \sum_{n=0}^{\infty} \frac{2\alpha\,(1+\alpha)}{1+\alpha+\alpha^2 q_n^2}\, exp\left\{-\frac{Dq_n^2\, t}{L2}\right\} \quad (5)$$

With

$$\alpha = \frac{1}{K_{P,F}} \frac{V_F}{V_P} \quad (6)$$

where: Mt. is the total amount of GA in food simulant at time t and M∞ is the total amount of GA in food simulant at the steady state, V_P is the polymer volume and V_F the food simulant volume, $(q_n)_n$, the positive roots of the equation tanq=−αq and $K_{P,F}$, the partition coefficient of the additive in the polymer/food simulant system.

The numerical simulations were carried out using Matlab® software and its lsqnonlin function to estimate the Dapp. For each model fitting, the quality of fit was estimated through the percentage of Root Mean Square Error (RMSE):

$$RMSE = \frac{1}{M_0}\sqrt{\frac{1}{N}\sum_{i=1}^{N}((M_t)experimental - (M_t)predicted)^2}\ \text{x}\ 100 \quad (7)$$

Where M_0 is the initial mass of GA in the film and M_t is the mass of GA into a food simulant at time t.

2.4.2 Modeling of O_2 absorption by gallic acid

Reaction model for GA powder:

The absorption kinetic was then depicted by an order 2 kinetic, as O_2 absorption depends on both scavenger and O_2 concentrations. As a simplification, partial orders were set to 1, leading to the following system of ODEs:

$$\frac{d[O_2]}{dt} = -nk[GA][O_2] \quad (8)$$

$$\frac{d[GA]}{dt} = -k[GA][O_2]$$

where $[O_2]$, is the concentration of O_2 in mol m^{-3}, [GA] is the concentration of GA in mol m^{-3}, n is the apparent stoichiometric coefficient for oxidation of GA by O_2 (%); and k is the kinetic coefficient in m^{-3} s^{-1} mol^{-1} for GA oxidation.

Reaction-diffusion model of GA introduced in PHBV film:

A reaction-diffusion system, similar to the one developed by Kombaya-Touckia-Linin et al., (2019), was used to describe the oxygen absorption by GA embedded in the film. The model described the diffusion of O_2 into the polymer matrix using Fick's law of diffusion and the reaction between O_2 and GA acording the equation (8).

It was assumed that : (i) GA was immobile into the polymer matrix; (ii) an homogeneous distribution of GA inside the film structure was achieved; (iii) the polymer was considered as homogeneous material with a single, constant, apparent O_2 diffusivity D_{O2} (m^2 s^{-1}).

The mathematical model for a plane film geometry reduced to the one-dimensional reaction–diffusion system is given in Equation (9), for x ∈]–L/2, L/2, where L is the thickness of the film:

$$\frac{\partial[O_2]\,(t,x)}{\partial t} = D_{O_2}\frac{\partial^2[O_2]}{\partial x^2} - k\,n[O_2](t,x)[GA](t,x)$$

$$\frac{\partial[GA]\,(t,x)}{\partial t} = -k\,[O_2](t,x)[GA](t,x) \qquad (9)$$

where k and n are the kinetic parameters previously determined for the powder.

The initial GA and O_2 concentrations, supposed uniform in the film were the following ones:

$$[GA](t_0) = \frac{x_{GA}^f\,\rho^f}{M_{GA}} \qquad (10)$$

$[O_2]\,(t_0) = 0$

Were x_{GA}^{f} represent the mass fraction of GA inside the active film (kilograms of gallic acid per kilogram of active film) ρ^{f} is the apparent density of PHBV (kg m^{-3}) and M_{GA} is the molar mass of GA (kg mol^{-1}). It was assumed that $[O_2]$ (t_0) =0.

The boundary conditions are similar to those described by Kombaya-Touckia-Linin et al., (2019).

$$D_{O_2}\frac{\partial[O_2]\,(t,x)}{\partial x}=\frac{\varphi_{L/2}}{A}=\frac{\varphi_{-L/2}}{A}=\frac{k}{RT}\left(P_{O_2,HS}-\frac{[O_2](t,x)}{K_H}\right)at\ x=(-)\frac{L}{2}and\forall t\geq 0 \quad (11)$$

Where T (K) is the temperature , R the ideal gas costant, $P_{O2,HS}$ (Pa) and $P_{O2,His}$ (Pa) are the oxygen partial pressure in the headspace and at the vicinity of the composite surface, respectively.

In equation (11) the external mass transfer coefficient k are reported using Biot number (Bi).

$$k=\frac{2B_iD_{O_2}}{L} \quad (12)$$

For the mass balance of oxygen into headspace it was assumeed that: (i) the film is isolated into a container with a constant headspace volume V_{HS} (m^3) (ii) the gas flow is negligible through the container. Therefore, the variation of the oxygen partial pressure is calculated as below:

$$\frac{\partial P_{O2,HS}}{\partial t}=k\frac{A}{V_{HS}}\left(2P_{O_2,HS}-\frac{[O_2](t,x=L/2)}{K_H}-\frac{[O_2](t,x=L/2)}{K_H}\right) \quad (13)$$

Numerical simulation were perfomed with a biot number ($Bi=10^5$). Equation (8) and (13) were transformed from a partial differential equation system into an ordinary differential equation (ODE) system by a spatial discretization with a second order cenral difference method and mesh of 100 nodes. The resulting ODE system was numericcaly solved using MATLAB (MathWorks).

3. Results and discusion

3.1 Impact of the thermoforming process on GA stability and distribution in PHBV film

292 PHBV/GA sheets were divided into four equal parts and GA contained in each part was quantified
293 after extraction. It was observed that a similar amount of GA (4.25±0.16 g GA /100 g of film) was
294 recovered from each part, indicating a good homogeneity of GA at the macromolecular level.
295 However, the total amount of GA extracted from the film sheet was only 85 ± 3% of the initial
296 amount introduced before the thermoforming process. Thus, the thermal process (3.5 min at 180°C
297 and cooling down in air) provoked 15% of GA mass loss, that could be attributed to thermal
298 degradation, and more specifically to oxidation as no volatile compounds could be produced at this
299 temperature (Alberti et al., 2016). Indeed, the thermal degradation of GA was already observed by
300 Ahn et al., (2016) and quantified by Santos et al., (2012). This latest measured a GA degradation of
301 9% at temperature range between 68°C and 213°C.
302 The apparent homogeneity of GA in PHBV matrix has been challenged by wide field microscopy
303 analysis. Images of the surface of the PHBV/GA films represented in Figure 1 (Figure 1B is a
304 close-up of Figure 1A) clearly showed that at the microscopic scale, the fluorescent GA which
305 emitted UV wave after excitation, appearing in yellow color; was not homogeneously distributed in
306 the polymer matrix. Furthermore, the numerous bubbles present on the surface of the film could be
307 attributed to the sodium carbonate that was not melted after film processing (tm = 850°C). Some
308 studies also reported heterogeneous dispersion of active compounds in polymer films, such as
309 thymol or eugenol in LDPE (Krepker et al., 2017; Goñi et al., 2016) or GA in chitosan (Rui et al.,
310 2017; Sun et al., 2014; Ahn et al., 2016). This heterogeneity depends mainly on the GA
311 concentration and nature of the interactions between the active compound and the polymer chains
312 (Rui et al., 2017). Indeed, GA at low concentrations was able to form hydrogen bounds with
313 polymer matrix; while at high concentrations a part of GA could remain unlinked, forming
314 aggregates.
315
316 **3.2 The antiradical activity of GA released into food simulants**

317 The concentration and percentage (equation 1) of GA diffused from PHBV film into aqueous food
318 simulant A and fatty food simulant D1 are shown in Figure.2. In contrast, GA was not released in
319 oily food simulant D2 (data not shown).
320 For both food simulants A and D1, the migration of GA increases with time and reaches a
321 maximum, point after which there is a slight decrease of GA concentration in food simulants, as a
322 result of oxidation of the GA diffused (combination of diffusion and oxidation, due to the
323 solubilization of oxygen in food simulants) (Figure 2). This oxidation lead to an underestimation of
324 the GA diffused in food simulants. GA migration is higher in food simulants D1 (511 mg/L after 5
325 days, corresponding to 39 % of the initial amount of GA present in the film) than in food simulant
326 A (384 mg/L after 8 day, corresponding to 31% of the initial GA present in the film), likely due to
327 the higher solubility of GA in ethanol compared to water (more than 30 times) (Daneshfar et al.,
328 2008; Noubigh et al., 2012). The same behaviour was observed for the migration of thymol which
329 was proportional to the amount of ethanol in the simulant (Tawakkal et al., 2016). Therefore, the
330 maximum release of GA is expected to occur in less polar foodstuffs, such as oil-in-water
331 emulsions (sauces, dressings or high-fat dairy products) and /or alcoholic beverages.
332 This increase of GA release in ethanol-rich medium was confirmed by the value of adjusted
333 apparent GA diffusivites in PHBV film, which is two time higher when the PHBV sheet is in
334 contact with food simulant D1 (6.48×10^{-14} m^2 s^{-1}) compared to food simulant A (3.58×10^{-14} m^2 s^{-1}).
335 The apparent diffusivity values identified for GA are in the same order of magnitude than those
336 found in the literature for other low molecular weight constituents. For example, Rubilar et al.,
337 (2017) identified a GA diffusivity between 3.7×10^{-14} and 6.1×10^{-14} m^2 s^{-1} from chitosan film into
338 water using a Fickian model. An acceptable fitting was observed between experimental data and
339 model with an average RMSE of 6.5% and 11.5% in food simulant A and D1 respectively. The
340 difference between model and experimental data was higher for the longer times, because the
341 diffusion of GA reached a plateau and oxidation that appeared during experiments was neglected in
342 model.

343 The released GA into food simulants A and D1displayed a significant inhibition of DPPH radical
344 and as expected, is ascribed to the total amount of GA released into the simulant. As depicted in
345 Figure 3, at maximum release, the percentage inhibition value (I%) was 68.7±0.1% and 77.5 ±0.1%
346 in simulant A and D1 respectively. In the case of food represented by simulant D1, the protection of
347 lipids against radical-induced oxidation would be effective. However, the antioxidant activity of
348 GA may not be exploited if the maximum daily intake is not respected.
349 The amount of GA released in contact with food simulants D1 and A, after 10 days, was about 377
350 ± 31 mg L^{-1} and 344 ± 4 mg L^{-1} respectively (Figure. 2 A, B) (corresponding to around 30 % of the
351 initial GA present in the film), while the amount of GA released in simulant D2 (isooctane) was
352 zero. Altough no Admissible Daily Intake (ADI) was estimated for gallic acid, the regulation
353 established the maximal acceptable ADI at 0.2 mg/kg of body weight for propyl gallate (a GA
354 ester), corresponding to 14 mg for an adult with an average body weight of 70 kg (FAO, 1976).
355 Assuming that GA would have a similar ADI value, the use of a conventionnal tray with 10g
356 weight (for 150g of food) containing 5% of GA whose 30% diffuses in food after 10 days
357 (simulants A and D1), will lead to the intake of 150 mg of GA for one adult (supposing he
358 consumed all the food), so 10 times higher than acceptable ADI. However, when a conventionnal
359 lid film with 1g weight is used, 15 mg of GA would diffuse into food, which is equivalent to the
360 maximal ADI. Consequently, the development of active material consisting of gallic acid should
361 only be permitted in trays at a concentration lower than 0.5% or in lid film at a concentration lower
362 than 5% for food corresponding to simulants A and D1.
363
364 **3.3 Oxygen absorption properties of the active PHBV film**
365 **3.3.1 Oxygen absorption capacities of GA/Na_2CO_3 powder**
366 The experimental kinetic of O_2 absorption capacity of the GA /Na_2CO_3 powder (2:1) at 23°C and
367 100% RH and the corresponding, calculated remaining active GA is displayed in Figure 4. After 15
368 days the cell was reopened in order to refill the headspace with oxygen, which is reflected by the

two cycles present in the figure. A maximal absorption capacity of 595 mg O_2 g^{-1} of GA was reached in 30 days. Indeed, in basic conditions, GA is indirectly a good oxygen scavenger because it has the capacity to donate four acidic protons and to form several forms of gallate radicals by consuming molecular oxygen (Pant et al., 2019). This maximal absorption capacity is slightly higher than the O_2 absorption capacity of 447 mg O_2 absorbed/ g of GA measured by Pant et al., (2017) using the same mixture composition at 21°C and 100% RH.

The mathematical model showed a good fitting performance to experimental data with a RMSE of 21.9 mg O_2 g^{-1} of GA. Table 1 showed the estimated values of kinetic coefficient k (7.8×10^{-7} m^3 mol^{-1} s^{-1}) and stoichiometric coefficient n (3.57). These parameter values are close to those found by (Pant et al., 2019) that used the same model on GA/ Na_2CO_3 powder (2:1) with a kinetic coefficient k of 1.496×10^{-6} m^3 mol^{-1} s^{-1} and a stoichiometric coefficient n of 2.53.

3.3.2 Oxygen absorption capacities of active film

The kinetic of O_2 absorption capacity of the GA /Na_2CO_3 (2:1) incorporated in PHBV film at 23°C and 100% RH and the calculated remaining active GA in film is reported in Figure 5. GA in PHBV film reached approximately the same maximal absorption capacity as in powder form, with an average value of 581 mg O_2 g^{-1} of GA. However, it took three times as long to reach this maximal absorption capacity (around 100 days for the film versus 30 days for the powder). Indeed, in the experiment with activated powder oxygen is directly in contact with GA, while in the PHBV/GA film, it must first be absorbed in the polymer matrix and then diffused into the polymer to reach GA, which consequently slows down its absorption kinetics. The diffusion-reaction mechanism is clearly O_2 diffusion rate-limiting.

The mathematical model used to simulate the oxygen absorption by GA present in the PHBV film integrated both : (i) the sorption and diffusion of oxygen in the PHBV film (diffusion part of the model) and (ii) the absorbtion kinetic of GA (reaction part of the model) (equation 9). Assuming that absorption kinetic of GA in its two forms (powder or embedded in film) is similar, the kinetic

395 (k) and stoichiometric (n) coefficients of the GA powder were used, i.e 7.8×10^{-7} m^3 mol^{-1} s^{-1} and
396 3.57 respectively. In litterature, the diffusivity value of oxygen D_{O2} in PHBV, or PHB ranges from
397 1.2×10^{-13} to 1.1×10^{-12} m^2 s^{-1} (Gupta et al., 2018; Crétois et al., 2014). To estimate the sorption of
398 oxygen S_{O2} (or k_h) in PHBV film, the permeability of the film was measured, its value being
399 $1.34\times10^{-17} \pm 1.66\times10^{-18}$ mol m^{-1} s^{-1} Pa^{-1} (table 1) , the S_{O2} was estimated by the relation S=P/D. It
400 ranged from 1.1×10^{-4} to 1.2×10^{-5} mol m^{-3} Pa^{-1} depending on the D value considered with the range
401 found in litterature. It was observed that for a same P_{O2} value (here 1.34×10^{-17} mol m^{-1} s^{-1} Pa^{-1}) the
402 oxygen absorption kinetic strongly depends on the couple of D_{O2} and S_{O2} used (Figure 5). For
403 example, on the first replica, the couple D_{O2} =1.2×10^{-13} m^2 s^{-1} and S_{O2} = 1.1×10^{-4} mol m^{-3} Pa^{-1}
404 allowed to reach an absorption capacity of 346 mg O_2 g^{-1} of GA after 123 days, while the couple
405 D_{O2} =1.1×10^{-12} m^2 s^{-1} and S_{O2} = 1.2×10^{-5} mol m^{-3} Pa^{-1} allowed to reach an absorption capacity of
406 211 mg O_2 g^{-1} of GA after 123 days (39% less than the previous case) (Figure 5). This result is
407 highlighting the importance to well determine both diffusivity and solubility values of oxygen into
408 PHBV to well predict the evolution of oxygen in active packaging headspace.
409 The model did not fit the experimental data for both replicates (Figure 5, P_{O2}=1.34×10^{-17} mol $m^{-1}s^{-1}$
410 Pa^{-1}), probably because of the modification of gas permeability due to the lack of active compound
411 homogeneity in the PHBV film (confirmed by microscopy analysis-Figure 1). The permeability of
412 PHBV film containing exhausted active compounds (5wt% of GA and 2.5 wt% of Na_2CO_3) was
413 measured. Unfortunately, measurement was unexploitable because of exceeded quantification
414 treshold. The excessively high oxygen increase during the permeability measurement confirms the
415 presence of pores in the active PHBV film. These results correlate with Ahn's observations (Ahn et
416 al., 2016) that the increase in GA/potassium carbonate from 1% to 20% in LDPE induces a
417 reduction of the intermolecular force between polymer chains, leading to the apparition of pores,
418 and consequently to the increase of gases permeability.
419 The oxygen permeability values of PHBV in litterature usually range from 1 to 7 $\times10^{-17}$ mol $m^{-1}s^{-1}$
420 Pa^{-1} (Berthet et al., 2016). In a last trial, the model simulating the oxygen absorption of GA in

PHBV film was run with the upper limit of this P_{O2} range, i.e. with the value of 7×10^{-17} mol m^{-1} s^{-1} Pa^{-1} , so 7 times higher than that measured in this study (with a S_{O2} range from 1.1×10^{-4} to 1.2×10^{-5} mol m^{-3} Pa^{-1} and a D_{O2} range from 5.9×10^{-12} to 6.3×10^{-13} mol m^{-3} Pa^{-1}). With this new permeability value, the model fited the experimental data for the first replica with the couple D_{O2} =6.3×10^{-13} m^2 s^{-1} and S_{O2} = 1.1×10^{-4} mol m^{-3} Pa^{-1}. The same couple of parameters also allowed to well reflect the experimental kinetic of cycle 2 and 3 for the second replica, the gap of 120 mg O_2 g^{-1} GA between experimental data and model accumulated in cycle 1, being maintained in the two following cycles. Therefore, these observations highlight that further research is needed to better understand and predict the absorption of oxygen by activated GA in polymer matrix.

4. Conclusion and recommendations for the use of PHBV/GA film as food packaging

In this study, active film based on PHBV/activated GA was developed. This film showed a promising capacity as both radical and oxygen scavenger and could be used as biodegradable packaging for different kinds of food.

In the case of contact with aqueous and some fatty food (food simulant A and D1) as meat, fish, or cheese, the GA amount present in the packaging should be lower than 0.5% in trays and could reach 5% in lid film, in the case of a food of 150 g (154 mL) packed in a 10g active tray (443 mL, of wich 289 mL of headspace) with 418 cm^2 of surface and 1g lid film with 256 cm^2 of surface. GA which does not diffuse into food could act as oxygen absorber, with an oxygen absorption capacity of 120 mg O_2 g^{-1} of GA after 10 days, corresponding to 7.7% of oxygen g^{-1} of GA for a volume of 289 mL. This oxygen absorption capacity could limit the oxygen entrance through the packaging and would enhance the benefit of oxygen-free modified atmosphere packaging by strengthening food protection against oxidation.

Since the GA does not diffuse into vegetable oil (food simulant D2, replaced by isooctane in this study), no restriction on the amount of GA in the packaging applied for this type of food

446 application. In this case, the protection from oxidation would performed thanks to the oxygen
447 absorption capacity of GA.
448 However, some improvements are still needed to find the right compromise between the amount of
449 GA needed for effective antioxidant activity and maintaining the structural integrity of the film.
450

451 **Declaration of Competing Interest**

452 The authors declare that they have no known competing financial interests or personal relationships
453 that could influence the work reported in this paper.

454

455 **Acknowledgments**

456 FG, FC, CA, and VG conceived and designed the experiments. FG, and FC performed the
457 experiments. FG, FC, CA, VG and ET analysed the data and wrote the paper. ET supervised the
458 work. The authos thank Geneviève Conéjéro, the responsible for MRI-PHIV Platform at CIRAD for
459 microscopy analyses.

460

461 **Funding sources**

462 The authors acknowledge the financial support by the Ministry of Education University and
463 Research (MIUR) in the frame of the National Operational Program ESF-ERDF Research and
464 Innovation 2014–2020, action I.1. Innovative PhD with industrial characterization.

465

466 **References**

467

468 Ahn, B. J., Gaikwad, K. K., & Lee, Y. S. (2016). Characterization and properties of LDPE film with

gallic-acid-based oxygen scavenging system useful as a functional packaging material. *Journal of Applied Polymer Science*, *133*(43), 1–8. https://doi.org/10.1002/app.44138

Alberti, A., Granato, D., Nogueira, A., Mafra, L.I., Colman, T.A.D., Schnitzler, E., 2016. Modelling the thermal decomposition of 3, 4, 5-trihydroxybenzoic acid using ordinary least square regression. *International Food Research Journal* 23, 30.

Angellier-Coussy, H., Guillard, V., Guillaume, C., & Gontard, N. (2013). Role of packaging in the smorgasbord of action for sustainable food consumption. *Agro Food Industry Hi-Tech*, *24*(3).

Aydogdu, A., Yildiz, E., Aydogdu, Y., Sumnu, G., Sahin, S., & Ayhan, Z. (2019). Enhancing oxidative stability of walnuts by using gallic acid loaded lentil flour based electrospun nanofibers as active packaging material. *Food Hydrocolloids*, *95*(April), 245–255. https://doi.org/10.1016/j.foodhyd.2019.04.020

Berthet, M.-A., Angellier-Coussy, H., Guillard, V., & Gontard, N. (2016). Vegetal fiber-based biocomposites: Which stakes for food packaging applications? *Journal of Applied Polymer Science*, *133*(2), n/a-n/a. https://doi.org/10.1002/app.42528

Berthet, M. A., Angellier-Coussy, H., Chea, V., Guillard, V., Gastaldi, E., & Gontard, N. (2015). Sustainable food packaging: Valorising wheat straw fibres for tuning PHBV-based composites properties. *Composites Part A: Applied Science and Manufacturing*, *72*, 139–147. https://doi.org/10.1016/j.compositesa.2015.02.006

Bossu, J., Angellier-Coussy, H., Totee, C., Matos, M., Reis, M., & Guillard, V. (2020). Effect of the Molecular Structure of Poly(3-hydroxybutyrate- co -3- hydroxyvalerate) (P(3HB-3HV)) Produced from Mixed Bacterial Cultures on Its Crystallization and Mechanical Properties. *Biomacromolecules*, *21*(4709–4723). https://doi.org/10.1021/acs.biomac.0c00826

Campo, M., Pinelli, P., & Romani, A. (2016). Hydrolyzable tannins from sweet chestnut fractions obtained by a sustainable and eco-friendly industrial process. *Natural Product Communications*, *11*(3), 409–415. https://doi.org/10.1177/1934578x1601100323

Cazón, P., Velazquez, G., Ramírez, J. A., & Vázquez, M. (2017). Polysaccharide-based films and

coatings for food packaging: A review. *Food Hydrocolloids*, *68*, 136–148. https://doi.org/10.1016/j.foodhyd.2016.09.009

Coffigniez, F., Matar, C., Gaucel, S., Gontard, N., & Guilbert, S. (2021). The Use of Modeling Tools to Better Evaluate the Packaging Benefice on Our Environment, *5*(April). https://doi.org/10.3389/fsufs.2021.634038

Crétois, R., Follain, N., Dargent, E., Soulestin, J., & Bourbigot, S. (2014). Microstructure and barrier properties of PHBV / organoclays bionanocomposites. *Journal of Membrane Science*, *467*, 56–66. https://doi.org/10.1016/j.memsci.2014.05.015

Daneshfar, A., Ghaziaskar, H. S., & Homayoun, N. (2008). Solubility of gallic acid in methanol, ethanol, water, and ethyl acetate. *Journal of Chemical and Engineering Data*, *53*(3), 776–778. https://doi.org/10.1021/je700633w

European Commission. (2011). Commission Regulation (EU) Nº 10/2011. *Of 14 January 2011 on Plastic Materials and Articles Intended to Come into Contact with Food. Official Journal of the European Union*, (L 12), 1–89.

FAO/WHO expert committee on Food Additives, Food and Agriculture Organization of the United Nations and World Health Organization (1976). Toxicological evaluation of certain food additives.

Gómez-Estaca, J., López-de-Dicastillo, C., Hernández-Muñoz, P., Catalá, R., & Gavara, R. (2014). Advances in antioxidant active food packaging. *Trends in Food Science and Technology*, *35*(1), 42–51. https://doi.org/10.1016/j.tifs.2013.10.008

Goñi, M. L., Gañán, N. A., Strumia, M. C., & Martini, R. E. (2016). Eugenol-loaded LLDPE films with antioxidant activity by supercritical carbon dioxide impregnation. *Journal of Supercritical Fluids*, *111*, 28–35. https://doi.org/10.1016/j.supflu.2016.01.012

Guillard, V., Gaucel, S., Fornaciari, C., Angellier-coussy, H., Buche, P., & Gontard, N. (2018). The Next Generation of Sustainable Food Packaging to Preserve Our Environment in a Circular Economy Context. *Frontiers in Nutrition*, *5*(December), 1–13.

https://doi.org/10.3389/fnut.2018.00121

Gupta, A., Mulchandani, N., Shah, M., Kumar, S., & Katiyar, V. (2018). Functionalized chitosan mediated stereocomplexation of poly(lactic acid): Influence on crystallization, oxygen permeability, wettability and biocompatibility behavior. *Polymer*, *142*, 196–208. https://doi.org/10.1016/j.polymer.2017.12.064

Hellwig, M. (2019). The Chemistry of Protein Oxidation in Food. *Angewandte Chemie - International Edition*, *58*(47), 16742–16763. https://doi.org/10.1002/anie.201814144

Kombaya-Touckia-Linin, E. M., Gaucel, S., Sougrati, M. T., Stievano, L., Gontard, N., & Guillard, V. (2019). Elaboration and characterization of active films containing iron-montmorillonite nanocomposites for O2 scavenging. *Nanomaterials*, *9*(9). https://doi.org/10.3390/nano9091193

Krepker, M., Shemesh, R., Danin Poleg, Y., Kashi, Y., Vaxman, A., & Segal, E. (2017). Active food packaging films with synergistic antimicrobial activity. *Food Control*, *76*, 117–126. https://doi.org/10.1016/j.foodcont.2017.01.014

Laguna, O., Durand, E., Baréa, B., Dauguet, S., Fine, F., Villeneuve, P., & Lecomte, J. (2020). Synthesis and evaluation of antioxidant activities of novel hydroxyalkyl esters and bis-aryl esters based on sinapic and caffeic acids. *Journal of Agricultural and Food Chemistry*, *68*(35), 9308–9318. https://doi.org/10.1021/acs.jafc.0c03711

Lajarrige, A., Gontard, N., Gaucel, S., Samson, M. F., & Peyron, S. (2019). The mixed impact of nanoclays on the apparent diffusion coefficient of additives in biodegradable polymers in contact with food. *Applied Clay Science*, *180*(January), 105170. https://doi.org/10.1016/j.clay.2019.105170

Licciardello, F., Wittenauer, J., Saengerlaub, S., Reinelt, M., & Stramm, C. (2015). Rapid assessment of the effectiveness of antioxidant active packaging-Study with grape pomace and olive leaf extracts. *Food Packaging and Shelf Life*, *6*, 1–6. https://doi.org/10.1016/j.fpsl.2015.08.001

Luzi, F., Pannucci, E., Santi, L., Kenny, J. M., Torre, L., Bernini, R., & Puglia, D. (2019). Gallic

547 acid and quercetin as intelligent and active ingredients in poly(vinyl alcohol) films for food
548 packaging. *Polymers*, *11*(12). https://doi.org/10.3390/polym11121999
549 Mohamed, S. A. A., El-Sakhawy, M., & El-Sakhawy, M. A. M. (2020). Polysaccharides, Protein
550 and Lipid -Based Natural Edible Films in Food Packaging: A Review. *Carbohydrate*
551 *Polymers*, *238*, 116178. https://doi.org/10.1016/j.carbpol.2020.116178
552 Noubigh, A., Jeribi, C., Mgaidi, A., & Abderrabba, M. (2012). Solubility of gallic acid in liquid
553 mixtures of (ethanol + water) from (293.15 to 318.15) K. *Journal of Chemical*
554 *Thermodynamics*, *55*, 75–78. https://doi.org/10.1016/j.jct.2012.06.022
555 Pant, A. F., Özkasikci, D., Fürtauer, S., & Reinelt, M. (2019). The Effect of Deprotonation on the
556 Reaction Kinetics of an Oxygen Scavenger Based on Gallic Acid, *7*(November), 1–7.
557 https://doi.org/10.3389/fchem.2019.00680
558 Pant, A. F., Sängerlaub, S., & Müller, K. (2017). Gallic Acid as an Oxygen Scavenger in Bio-Based
559 Multilayer Packaging Films. *Materials*, *10*(489). https://doi.org/10.3390/ma10050489
560 Radi, M., Firouzi, E., Akhavan, H., & Amiri, S. (2017). Effect of gelatin-based edible coatings
561 incorporated with Aloe vera and black and green tea extracts on the shelf life of fresh-cut
562 oranges. *Journal of Food Quality*, *2017*. https://doi.org/10.1155/2017/9764650
563 Rouméas, L., Billerach, G., Aouf, C., Dubreucq, É., & Fulcrand, H. (2018). Furylated Flavonoids:
564 Fully Biobased Building Blocks Produced by Condensed Tannins Depolymerization. *ACS*
565 *Sustainable Chemistry and Engineering*, *6*(1), 1112–1120.
566 https://doi.org/10.1021/acssuschemeng.7b03409
567 Rubilar, J. F., Cruz, R. M. S., Zuñiga, R. N., Khmelinskii, I., & Vieira, M. C. (2017). Mathematical
568 modeling of gallic acid release from chitosan films with grape seed extract and carvacrol.
569 *International Journal of Biological Macromolecules*, *104*, 197–203.
570 https://doi.org/10.1016/j.ijbiomac.2017.05.187
571 Rui, L., Xie, M., Hu, B., Zhou, L., Yin, D., & Zeng, X. (2017). A comparative study on
572 chitosan/gelatin composite films with conjugated or incorporated gallic acid. *Carbohydrate*

Polymers, *173*, 473–481. https://doi.org/10.1016/j.carbpol.2017.05.072

Sanches-Silva, A., Costa, D., Albuquerque, T. G., Buonocore, G. G., Ramos, F., Castilho, M. C., … Costa, H. S. (2014). Trends in the use of natural antioxidants in active food packaging: a review. *Food Additives and Contaminants - Part A Chemistry, Analysis, Control, Exposure and Risk Assessment*, *31*(3), 374–395. https://doi.org/10.1080/19440049.2013.879215

Santos, N. A., Cordeiro, A. M. T. M., Damasceno, S. S., Aguiar, R. T., Rosenhaim, R., Carvalho Filho, J. R., … Souza, A. G. (2012). Commercial antioxidants and thermal stability evaluations. *Fuel*, *97*, 638–643. https://doi.org/10.1016/j.fuel.2012.01.074

Singh, G., Singh, S., Kumar, B., & Gaikwad, K. K. (2020). Active barrier chitosan films containing gallic acid based oxygen scavenger. *Journal of Food Measurement and Characterization*, (0123456789). https://doi.org/10.1007/s11694-020-00669-w

Sun, X., Wang, Z., Kadouh, H., & Zhou, K. (2014). The antimicrobial, mechanical, physical and structural properties of chitosan-gallic acid films. *LWT - Food Science and Technology*, *57*(1), 83–89. https://doi.org/10.1016/j.lwt.2013.11.037

Tawakkal, I. S. M. A., Cran, M. J., & Bigger, S. W. (2016). Release of thymol from poly(lactic acid)-based antimicrobial films containing kenaf fibres as natural filler. *LWT - Food Science and Technology*, *66*, 629–637. https://doi.org/10.1016/j.lwt.2015.11.011

Vermeiren, L., Devlieghere, F., Van Beest, M., De Kruijf, N., & Debevere, J. (1999). Developments in the active packaging of foods. *Trends in Food Science and Technology*, *10*(3), 77–86. https://doi.org/10.1016/S0924-2244(99)00032-1

Wang, Y., Du, H., Xie, M., Ma, G., Yang, W., Hu, Q., & Pei, F. (2019). Characterization of the physical properties and biological activity of chitosan films grafted with gallic acid and caffeic acid: A comparison study. *Food Packaging and Shelf Life*, *22*(September). https://doi.org/10.1016/j.fpsl.2019.100401

Wanner, G.T., 2010. O2 -zehrende und -anzeigende Packstoffe für Lebensmittelverpackungen. Technische Universität Munich.

Figures (from 1 to 5)

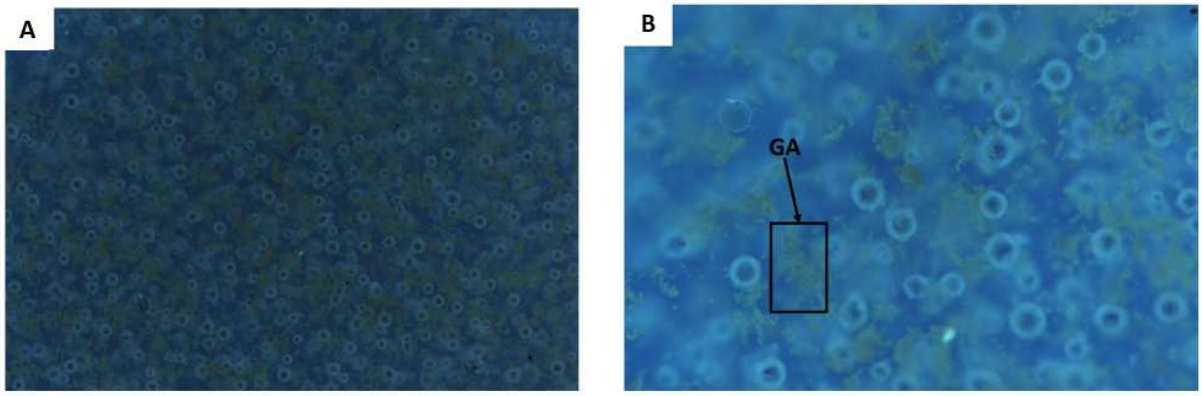

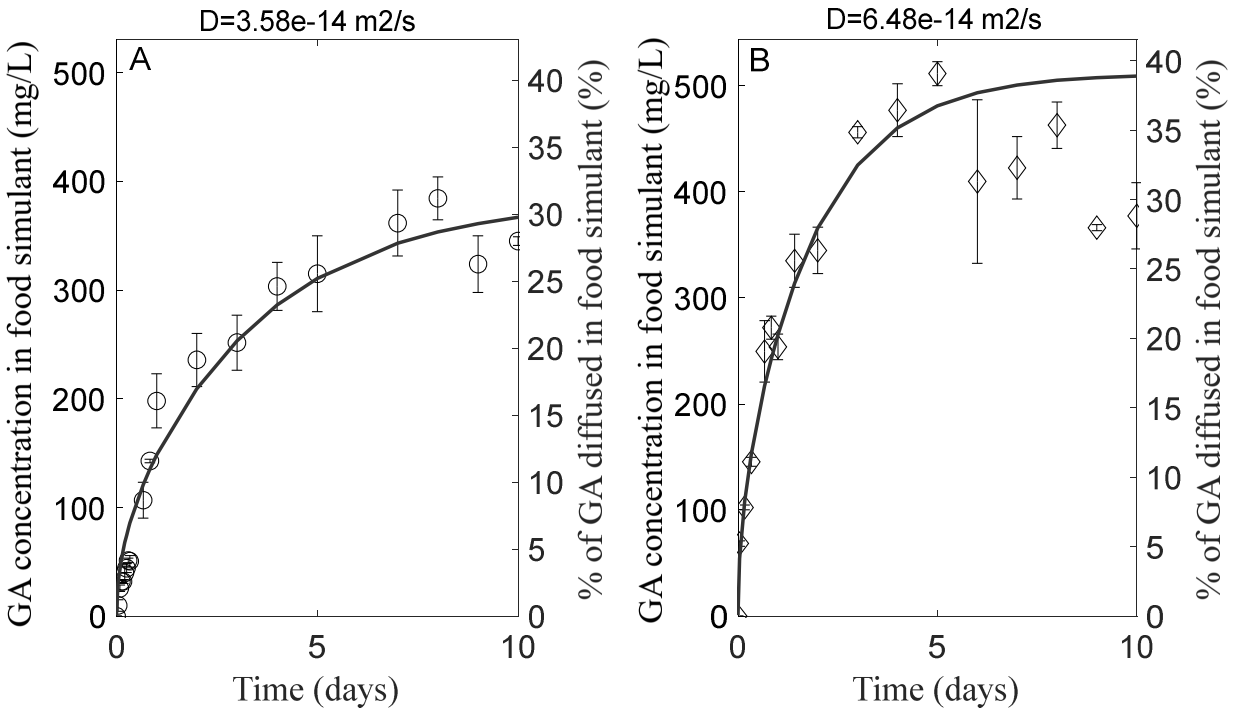
D=3.58e-14 m2/s
A
GA concentration in food simulant (mg/L)
% of GA diffused in food simulant (%)
Time (days)
D=6.48e-14 m2/s
B
GA concentration in food simulant (mg/L)
% of GA diffused in food simulant (%)
Time (days)

603
604

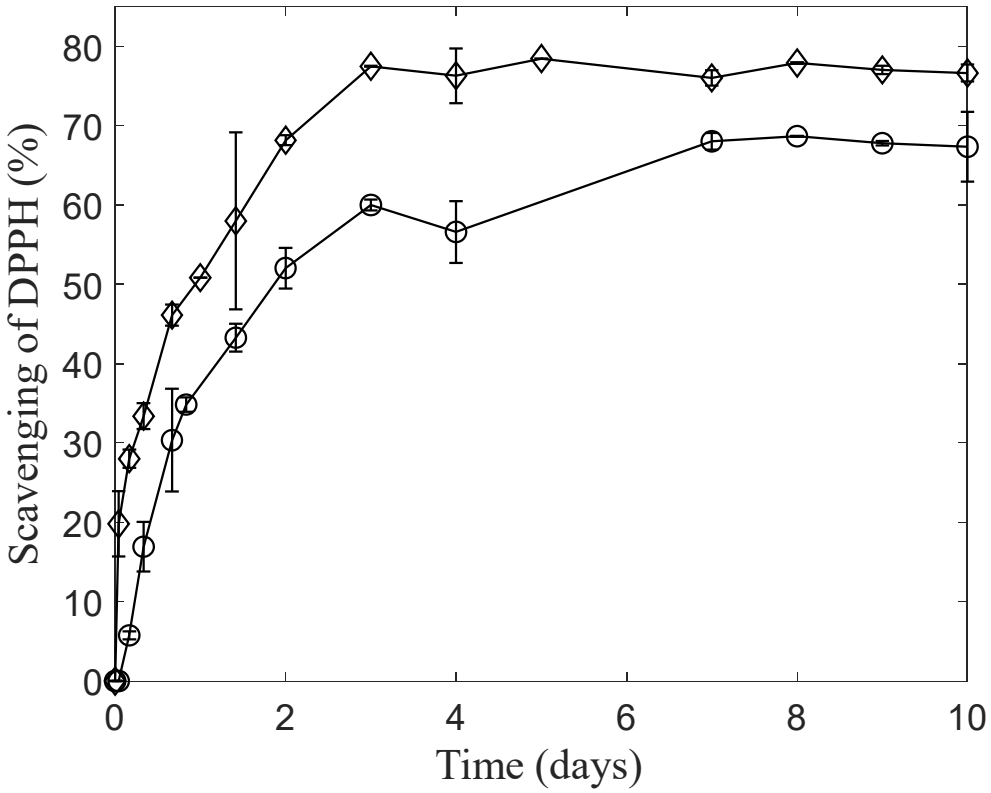

605
606

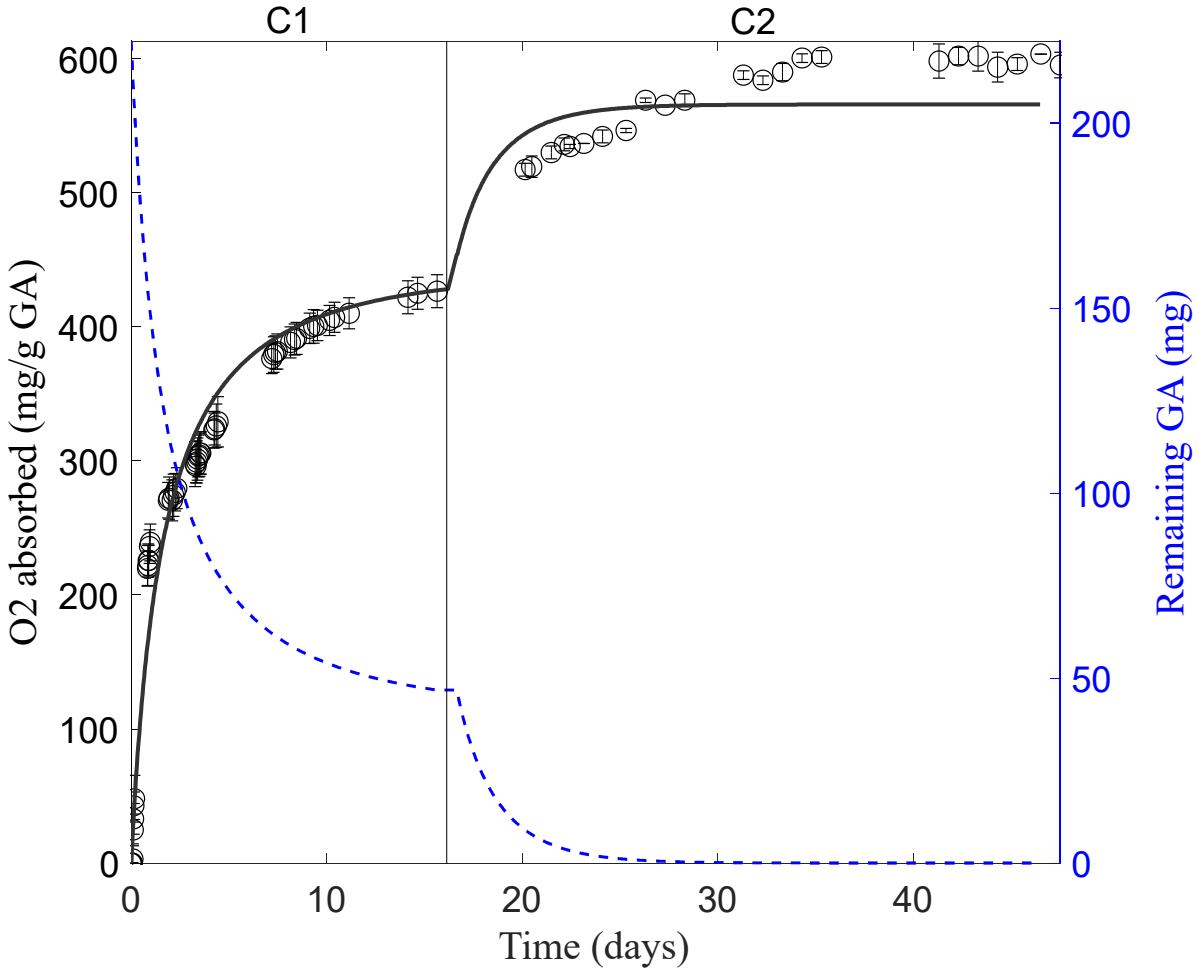
C1
C2
O2 absorbed (mg/g GA)
Remaining GA (mg)
Time (days)
0
100
200
300
400
500
600
0
50
100
150
200
0
10
20
30
40

607
608

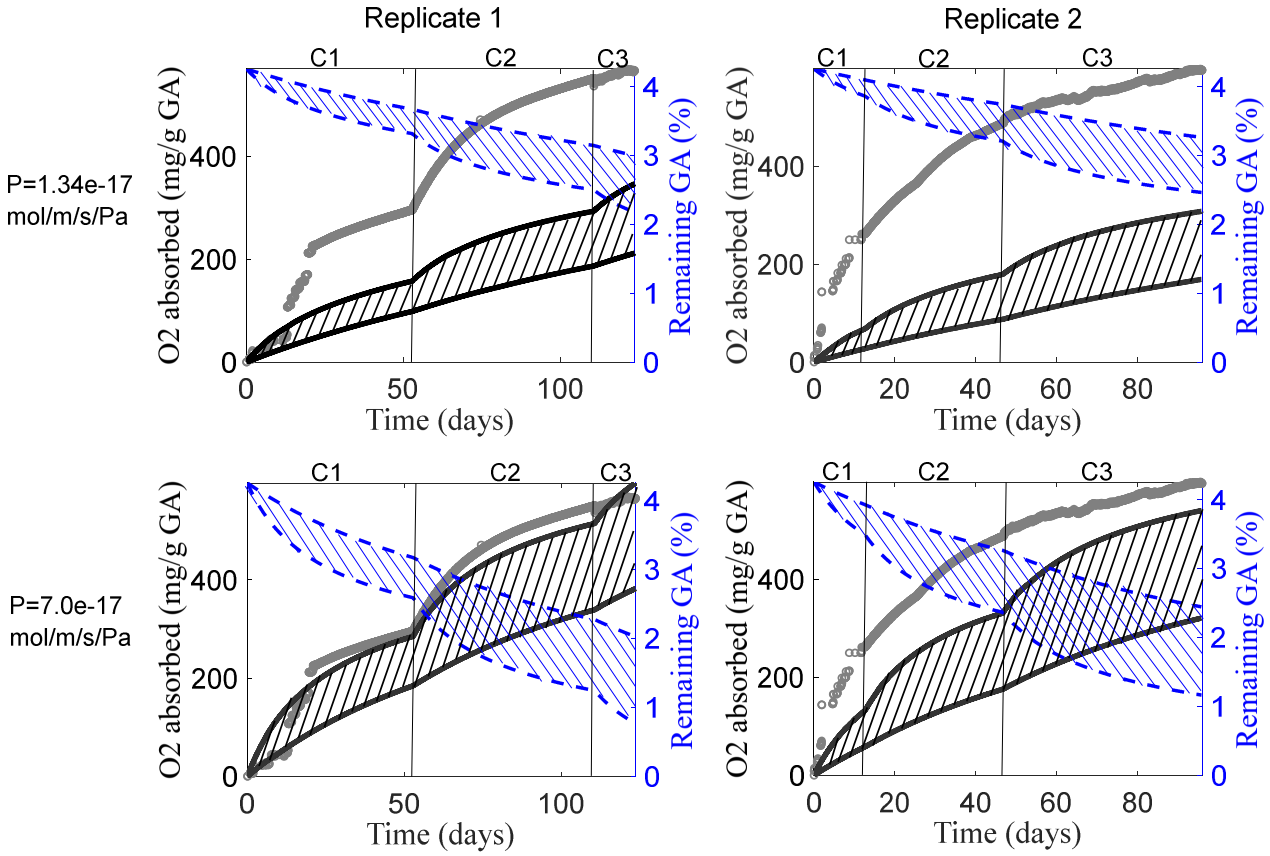
Replicate 1
Replicate 2
P=1.34e-17
mol/m/s/Pa
P=7.0e-17
mol/m/s/Pa
C1
C2
C3
O2 absorbed (mg/g GA)
Remaining GA (%)
Time (days)
0
200
400
0
1
2
3
4
0
50
100
0
20
40
60
80

609

610 **Table**

O_2 absorption by gallic acid				
Sample	**k ($m^3mol^{-1}s^{-1}$)**	**n**	**Conditions**	**Reference**
GA/Na_2CO_3 powder in ratio 2 :1	7.8×10^{-7}	3.87	23°C and 100% RH	This study

O_2 barrier properties of PHBV					
Sample	**Permeability (mol $m^{-1}s^{-1}Pa^{-1}$)**	**Diffusivity (m^2s^{-1})**	**Solubility (mol $m^{-3}Pa^{-1}$)**	**Conditions**	**Reference**
PHBV	1.34×10^{-17}	-	Estimated from $S=P\times D=1.12\times10^{-4}$	23°C and 50% RH	This study
PHBV	Not use	1.2×10^{-13}		23°C and 0% RH	Crétois *et al*, 2014
PHB	Not use	1.1×10^{-12}	Estimated from $S=P\times D=1.22\times10^{-5}$	24°C and 80% RH	Sanchez-Garcia *et al*, 2008

611

612 **Figure captions**
613

614 **Figure 1**: Wide-field microscopy of PHBV-GA films of 1 cm width and 200µm thickness, with
615 10X Plan APO objective. Image 1B is a close-up of image 1A.

616

617 **Figure 2**: Migration of GA (mg/mL or %) from PHBV film into food simulant A (10% ethanol) (A)
618 and food simulant D1 (50% ethanol) (B) at 25°C. Dots and line represented experimental data and
619 model data respectively. The error bars represent the standard deviation (n=3).

620

621 **Figure 3**: Kinetic of DPPH radical scavenging activity after migration of GA in food simulant A,
622 ie 10% ethanol (circle) and D1, ie 50% ethanol (diamond). The error bars represent the standard
623 deviation (n=2)

624

625 **Figure 4**: Experimental (dots) and predicted (black line) O_2 absorption capacities of gallic acid
626 /Na_2CO_3 powder (2:1) (mg O_2/g of GA) at 23°C and 100% RH and predicted consumption rate of
627 gallic acid /Na_2CO_3 powder (2:1) at the same condition (blue dotted line). Between cycle 1 (C1) and
628 cycle 2 (C2), the jar was reopened to recharge the headspace in oxygen. The error bars represent
629 the standard deviation (n=3)

630

631 **Figure 5**: Experimental (dots) and predicted (black line) O_2 absorption capacities of
632 PHBV/GA(5%)/ Na_2CO_3(2.5%) film at 21° and 100% RH; and predicted consumption rate of the
633 film at the same condition (blue dotted line) for two replicates (one at right and one at left) and with
634 two different values of O_2 permeability (1.34×10^{-17} mol/m/s/Pa up and 7.0×10^{-17} mol/m/s/Pa
635 down). For each P_{O2} value, two couple of D_{O2} and S_{O2} in PHBV film were tested to represent the
636 predicted absorption capacities (black line) that were joined by cross hatch. Between cycle 1 (C1)

637 and cycle 2 (C2); and between cycle 2 (C2) and cycle 3 (C3), the jar was reopened to recharge the
638 headspace in oxygen.
639
640 **Table 1**: Values of parameters used in the oxygen absorption capacity model of PHBV containing
641 5% of GA and 2.5% of Na_2CO_3 film.
642

Highlights

- PHBV films containing 5% of GA and 2.5% of Na_2CO_3 were produced by thermoforming.
- 30% of GA diffused in food simulant A and D1, leading to high radical inhibition.
- Maximal O_2 absorption capacity reached 581 mg O_2/g of GA for active film.
- Migration of GA in food simulant and O_2 absorption by GA were successfully modelled.
- Results could be used to design active packaging protecting food from oxidation.